Hum Genet (2016) 135:909–917
DOI 10.1007/s00439-016-1685-3

ORIGINAL INVESTIGATION

De novo *RRAGC* mutation activates mTORC1 signaling in syndromic fetal dilated cardiomyopathy

Pamela A. Long[1,2] · Michael T. Zimmermann[3] · Maengjo Kim[4] · Jared M. Evans[3] · Xiaolei Xu[4,6] · Timothy M. Olson[2,5,6]

Received: 1 March 2016 / Accepted: 14 May 2016 / Published online: 27 May 2016

Abstract Idiopathic dilated cardiomyopathy (DCM) is a heritable, genetically heterogeneous disorder with variable age-dependent penetrance. We sought to identify the genetic underpinnings of syndromic, sporadic DCM in a newborn female diagnosed in utero. Postnatal evaluation revealed ventricular dilation and systolic dysfunction, bilateral cataracts, and mild facial dysmorphisms. Comprehensive metabolic and genetic testing, including chromosomal microarray, mitochondrial DNA and targeted RASopathy gene sequencing, and clinical whole exome sequencing for known cardiomyopathy genes was non-diagnostic. Following exclusion of asymptomatic DCM in the parents, trio-based whole exome sequencing was carried out on a research basis, filtering for rare, predicted deleterious de novo and recessive variants. An unreported de novo S75Y mutation was discovered in *RRAGC*, encoding Ras-related GTP binding C, an essential GTPase in nutrient-activated mechanistic target of rapamycin complex 1 (mTORC1) signaling. In silico protein modeling and molecular dynamics simulation predicted the mutation to disrupt ligand interactions and increase the GDP-bound state. Overexpression of $RagC^{S75Y}$ rendered AD293 cells partially insensitive to amino acid deprivation, resulting in increased mTORC1 signaling compared to wild-type RagC. These findings implicate mTORC1 dysregulation through a gain-of-function mutation in RagC as a novel molecular basis for syndromic forms of pediatric heart failure, and expand genotype–phenotype correlation in RASopathy-related syndromes.

M. T. Zimmermann and M. Kim contributed equally to this work.

Electronic supplementary material The online version of this article (doi:10.1007/s00439-016-1685-3) contains supplementary material, which is available to authorized users.

✉ Timothy M. Olson
olson.timothy@mayo.edu

[1] Mayo Graduate School, Molecular Pharmacology and Experimental Therapeutics Track, Mayo Clinic, Rochester, MN, USA

[2] Cardiovascular Genetics Research Laboratory, Mayo Clinic, Stabile 5, 200 First Street SW, Rochester, MN 55905, USA

[3] Division of Biomedical Statistics and Informatics, Department of Health Sciences Research, Mayo Clinic, Rochester, MN, USA

[4] Department of Biochemistry and Molecular Biology, Mayo Clinic, Rochester, MN, USA

[5] Division of Pediatric Cardiology, Department of Pediatric and Adolescent Medicine, Mayo Clinic, Rochester, MN, USA

[6] Division of Cardiovascular Diseases, Department of Internal Medicine, Mayo Clinic, Rochester, MN, USA

Introduction

Dilated cardiomyopathy (DCM), a progressive heritable disorder leading to heart failure and premature death, is the most common indication for cardiac transplantation (Olson and Chan 2013). The mean age at diagnosis is 45 years (Michels et al. 1992), but a subset of patients become clinically symptomatic in childhood. Furthermore, some children develop DCM and advanced heart failure in the absence of myocardial disease in their adult parents (Long et al. 2015a; b). Diagnosis of sporadic DCM in an infant or child should prompt a broad differential diagnosis and testing for reversible causes of heart failure, yet it remains an idiopathic disorder in 66 % of children (Towbin et al. 2006). DCM gene discovery has traditionally depended on locus mapping in familial cases (Brauch et al. 2009),

posing a challenge to decipher the role of genetics in the pathogenesis of sporadic DCM (Hershberger et al. 2010). Mutations in over 50 genes are known to cause DCM (Hershberger et al. 2013; Olson and Chan 2013), yet the yield of commercial genetic testing panels in DCM is only 37 % (Pugh et al. 2014). Whole exome sequencing (WES) is a transformative technology with the potential to accelerate novel gene discovery in children with sporadic DCM.

Methods

Study subjects

Subjects provided written informed consent under a research protocol approved by the Mayo Clinic Institutional Review Board and were phenotypically classified by transthoracic echocardiography. Diagnostic criteria for DCM were left ventricular diastolic and/or systolic short-axis chamber dimension Z-score ≥2.0, and left ventricular ejection fraction <50 %. Genomic deoxyribonucleic acid (DNA) was isolated from peripheral-blood white cells.

Whole exome sequencing and bioinformatics

WES and variant annotation were performed on DNA samples from the family trio, utilizing the Mayo Clinic Medical Genome Facility and Bioinformatics Core. The Agilent SureSelect Human All Exon v5+UTRs capture kit (Agilent) was used for exome capture. Samples were multiplexed on a single lane and 101 base pair, paired-end sequencing was performed on Illumina's HiSeq 2000 platform (Illumina, Inc). Reads were aligned to the hg19 reference genome with Novoalign (http://novocraft.com) followed by sorting and marking of duplicate reads using Picard (http://picard.sourceforge.net). Local realignment of insertions/deletions (INDELs) and base quality score recalibration were then performed using the Genome Analysis Toolkit (GATK) (McKenna et al. 2010). Single nucleotide variants (SNVs) and INDELs were called across all three samples simultaneously using GATK's UnifiedGenotyper with variant quality score recalibration (DePristo et al. 2011). The resultant variant call format files were analyzed with QIAGEN's Ingenuity® Variant Analysis™ software. To identify true-positives, WES and whole genome sequencing (WGS) data from 115 in-house individuals not affected with DCM were utilized. To determine rarity of variants, minor allele frequencies from three publicly available databases were used: 1000 Genomes (WGS data from 1092 individuals). (The 1000 Genomes Consortium 2012), Exome Variant Server (EVS, WES data from 6503 individuals) (http://evs.gs.washington.edu/EVS/), or the Exome Aggregation Consortium (ExAC, WES data from 60,706 individuals) (http://exac.broadinstitute.org). Non-paternity was excluded by calculating the identity by decent (IBD) probabilities with Prest-plus (Sun and Dimitromanolakis 2014) using a set of 43,700 autosomal SNVs with a read depth of at least 10 and a 1000 Genomes minor allele frequency of 30 % or greater.

Molecular dynamics simulations

Generalized Born implicit solvent molecular dynamics (isMD) simulations were carried out using NAMD (Phillips et al. 2005) and the CHARMM22 with CMAP (Mackerell et al. 2004) force field. An interaction cutoff of 15Å and time step of 1 fs was used in all simulations with conformations recorded every 2 ps. Due to increased kinetics from lack of solvent friction and occlusion, time is functionally accelerated in isMD.

The PDB structure 3LLU (Nedyalkova et al. 2010) was utilized for the initial conformation. Conformations for S75Y and S75L were generated from 3LLU by computational mutagenesis, selecting the rotamer with least steric clash. GDP and GTP ligand parameters were gathered from the ZINC database (ZINC IDs 8215481 and 53684323, respectively) (Irwin et al. 2012) and aligned to the GNP (non-hydrolyzable GTP analog) of 3LLU using PyMOL (The PyMOL Molecular Graphics System. Version 1.5.0.3: Schrödinger, LLC). Combinations of the three sequence contexts (WT, S75Y, and S75L) and three ligand states (apo, GDP, and GTP) made for nine independent simulations. Each of these nine initial conformations was energy minimized for 10,000 steps followed by heating to 300 K over 300 ps via a Langevin thermostat. They were equilibrated for 21 ns and a further 80 ns was used in analysis.

Trajectory analysis

All trajectories were first aligned to the initial apo-WT conformation using C_α atoms. Root mean squared deviation (RMSD) was calculated using only C_α atoms. Due to the large number of frames/conformations analyzed, all distributions differed from each other with statistical significance ($p < 10^{-12}$). Therefore, we generated conservative p values for comparing RMSD distributions by randomly subsampling each trajectory to 100 frames and compared them using t tests, utilizing the least significant p value observed across 10,000 random iterations. Principal component (PC) analysis was performed in Cartesian space. Analysis was carried out using custom scripts, leveraging the Bio3D R package (Grant et al. 2006).

Cell culture and immunoblotting

AD293 cells (Agilent) were cultured in DMEM medium in the presence of 10 % FBS and 100 U/mL penicillin/100 μg/mL streptomycin. Human *RRAGC* cDNA was synthesized from total RNA of normal human adult heart (Biochain) by RT-PCR and cloned into a pshuttle-IRES-GFP vector (Agilent). The S75Y missense mutation was introduced into *RRAGC* cDNA according to the GeneArt site-directed mutagenesis system (Thermofisher). AD293 cells were transfected with plasmid constructs expressing control-GFP (empty vector), wild-type (WT) RagC, or $RagC^{S75Y}$ using Lipofectamine 2000 (Thermofisher). Forty-eight hours after transfection, cells were starved of amino acids and FBS for 50 min, and then re-stimulated in DMEM alone for 20 min. Protein samples were prepared from treated cells using lysis buffer containing protease inhibitors (Sigma). After adjustment of protein concentration, cell lysates were loaded and separated in an SDS-PAGE gel, which was transferred onto a polyvinylidene difluoride membrane (Bio-Rad Laboratories). Membranes were blocked in 5 % non-fat milk and incubated with primary antibodies overnight at 4 °C. The following primary antibodies were used: RagC (#5466; Cell Signaling Technology), Phospho-p70 S6Kinase (T389, #9234; Cell Signaling Technology), p70 S6Kinase (#2708; Cell Signaling Technology), Phospho-S6 ribosomal protein (S40/244, #2215; Cell Signaling Technology), S6 ribosomal protein (#2217; Cell Signaling Technology), β-actin (#A3854; Sigma), and GFP (#240141; Agilent). Membranes were incubated with appropriate secondary antibodies conjugated to horseradish peroxidase (HRP) (Santa Cruz) and signals were visualized by Chemiluminescence (GE Healthcare). Three independent experiments were conducted and densities of the immunoreactive bands were evaluated using NIH Image software. Statistical analysis was performed using Student's *t* test.

Results

Clinical presentation of syndromic, fetal dilated cardiomyopathy

A 22-month-old female of white European ancestry was diagnosed with fetal cardiomegaly at 30 weeks gestation and delivered 1 week later for fetal hydrops. Postnatal echocardiography revealed severe biventricular and biatrial chamber enlargement, severe systolic dysfunction (left ventricular ejection fraction (LVEF) 25 %; normal >50 %), a small apical ventricular septal defect, and a moderate secundum atrial septal defect. Mild facial dysmorphism (wide-set eyes, down-slanted palpebral fissures, prominent forehead, mild macrocephaly, low-set ears) and bilateral cataracts were also identified. Her Minnesota newborn screen for inborn errors of metabolism was negative. An extensive diagnostic workup was performed, including further metabolic pathway testing (plasma lactate and pyruvic acid, plasma uric acid, plasma carnitine and acylcarnitine profile, glycosylation profile, urine organic acids, creatine kinase, peroxisomal panel), karyotyping, chromosomal microarray, mitochondrial DNA and targeted RASopathy gene sequencing, and ultimately clinical WES, none of which uncovered the molecular basis for her DCM. Parental screening echocardiograms excluded asymptomatic DCM (father: 33 years; mother: 33 years). The patient was hospitalized for 2 months for treatment of prematurity and heart failure, with gradual improvement in systolic function on medical therapy (LVEF 50 %) enabling transition from a continuous milrinone infusion to oral digoxin and captopril therapy. At 4 months of age, a gastrostomy tube was placed for oral aversion and failure to thrive. The patient suffered a gradual decline in cardiac function, necessitating two hospital admissions at 21 months of age for decompensated heart failure (LVEF 22 %) with severe biatrial enlargement indicative of restrictive physiology. A potential metabolic disorder was suspected due to hypoglycemia (nadir glucose 13 mg/dL, normal 70–140) and elevated lactate (peak lactate 5.4 mmol/L, normal 0.6–3.2) and hepatic transaminase levels (peak AST 7319 U/L, normal 8–50; peak ALT 3290 U/L, normal 7–45) upon each admission, yet skin and skeletal muscle biopsies excluded abnormalities in respiratory chains (Table S1), mitochondrial DNA sequence and content, and tissue ultrastructure. These laboratory derangements, which were transient and had not been present in the neonatal period, were ultimately attributed to low cardiac output and congestive hepatopathy. The patient was enrolled in our research study for DCM gene discovery and died shortly thereafter at 22 months of age with intractable multisystem organ failure due to severe, end-stage heart failure.

Exome sequencing uncovers de novo RRAGC mutation

Prior to enrollment in our study, patient-only WES was performed in a clinical diagnostics laboratory, utilizing parental DNA to test for inheritance by Sanger sequencing. All known disease genes related and unrelated to the patient's clinical phenotype were interrogated (Richards et al. 2007), but no actionable mutations were reported. Trio-based WES (Fig. 1a) was then carried out on a research basis to identify rare protein coding variants among all genes, regardless of previous disease associations. Parent–proband relationships were confirmed with Prest-plus (Table S2) (Sun and Dimitromanolakis 2014). All 3 samples had over 97 % of reads map to the hg19 reference genome and, on average, 96 % of the 74.86 megabase capture region had ≥20× coverage.

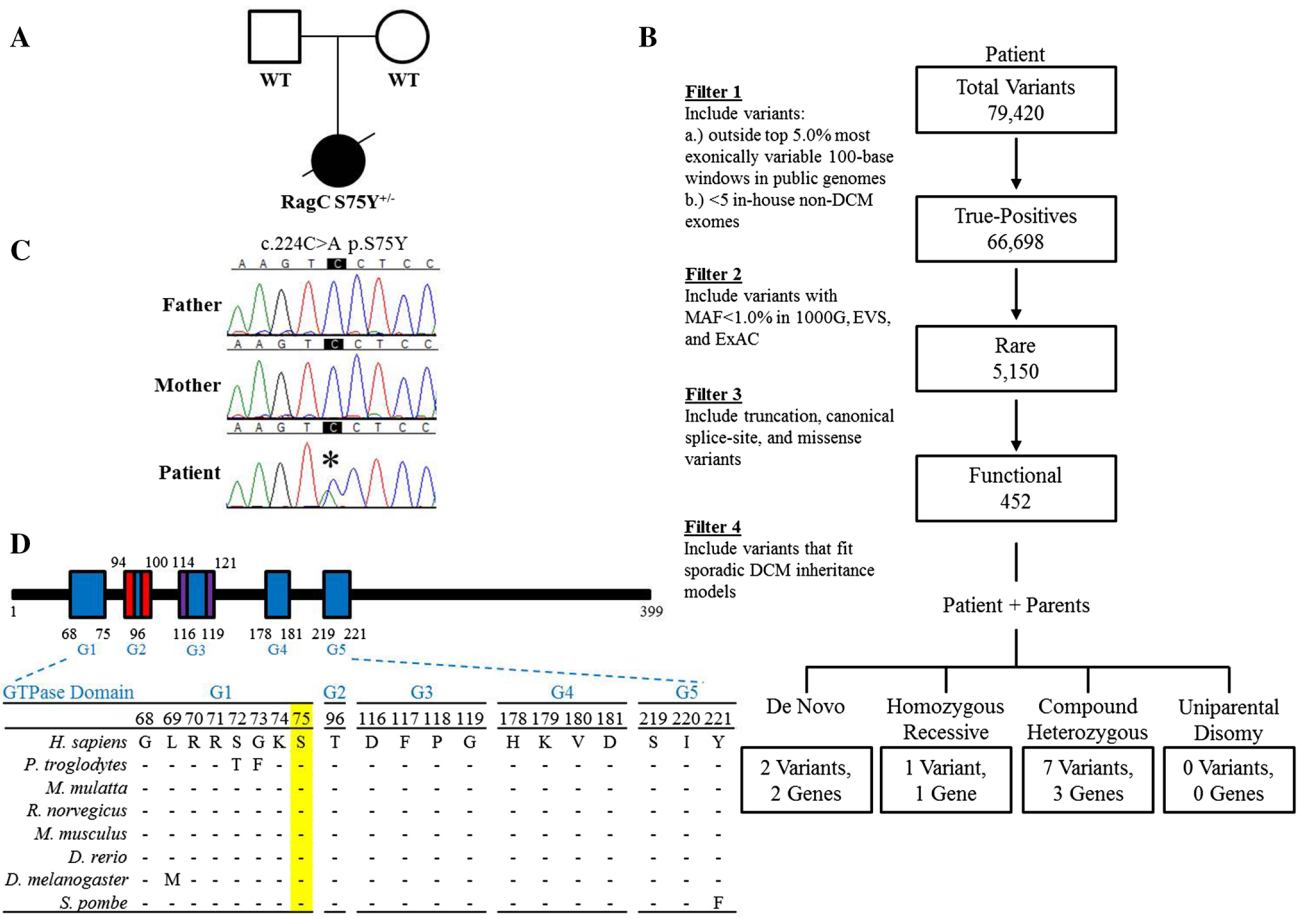

Fig. 1 Whole exome sequencing reveals de novo RagC S75Y mutation. **a** Family pedigree of sporadic DCM. *Square* male, *circle* female, *solid* affected, *open* unaffected, *slash* deceased. **b** Iterative filtering identified ten candidate variants in six genes. *1000G* 1000 Genomes, *DCM* dilated cardiomyopathy, *EVS* Exome Variant Server, *ExAC* the Exome Aggregation Consortium, *MAF* minor allele frequency. **c** Sanger sequencing of *RRAGC* confirmed the c.224C>A, p.S75Y de novo mutation. **d** The GTPase domain, comprising G1–G5, is highly conserved. S75 resides within G1, also known as the P-loop. *Dashes* conserved residues, *blue* GTPase domain, *red* switch I region, *purple* switch II region (color figure online)

On average, 75,000 SNVs and 9300 INDELs were identified in the coding region of each sample, which was within an expected range for our standard variant calling workflow. To identify a pathogenic mutation, an iterative variant filtering approach was then employed (Fig. 1b). Variants that mapped to the coding region and passed quality score recalibration were filtered to exclude those outside the top 5.0 % of most exonically variable 100-base windows in healthy public genomes (The 1000 Genomes Consortium 2012) and those present in three or more in-house, non-DCM controls. Variants were then filtered for rarity, excluding those with a minor allele frequency ≥1.0 % in 1000 Genomes, EVS, or ExAC. Next, all missense, truncation, and canonical splice-site variants were retained. Filtered data from the patient were analyzed in conjunction with parental WES data to model all potential modes of inheritance for sporadic DCM, including de novo, homozygous recessive, compound heterozygous, and uniparental disomy, culminating in a candidate list of ten variants in six genes (Table S3). Systematic examination of each variant/gene (Supplementary Information) revealed a de novo missense mutation in *RRAGC* (Online Mendelian Inheritance in Man #608267), encoding Ras-related GTP-binding protein C that functions as a molecular switch for nutrient-activated mTORC1 signaling (Fig. 1a–c). While synergistic heterozygosity involving one or more of the identified candidate variants cannot be excluded as contributing to the disease phenotype, the resultant c.224C>A, p.S75Y (NM_022157.3) substitution in *RRAGC*, predicted damaging by SIFT and PolyPhen2 (Adzhubei et al. 2010; Kumar et al. 2009), remained as the single most plausible candidate. The de novo missense mutation occurred in the highly conserved GTPase-binding domain (Fig. 1d) and was absent in the ExAc database. Further, there was complete absence of missense and truncating variants in the GTPase-binding domain of *RRAGC* among ExAC controls.

RagC^{S75Y} disrupts ligand interactions

Previous random mutagenesis studies of the small GTPase, Ras, identified a Ras^{GDP}-bound mutant, Ras^{S17N}, resulting in dominant negative inhibition of endogenous Ras activation (Feig and Cooper 1988). Homology studies of the invariantly conserved P-loop Ser17 residue in GTP-binding proteins guided synthetic engineering of a RagC P-loop mutant, RagC^{S75L}, which alters the same Ser75 residue mutated in our patient. RagC^{S75L} is routinely used to model the RagC^{GDP}-bound state, necessary for amino acid activation of mTORC1 (Sancak et al. 2008). To predict the molecular impact of the RagC^{S75Y} mutation identified in our patient, in silico protein modeling and molecular dynamics simulations were carried out in parallel with the functionally characterized RagC-GDP^{S75L} mutation. These analyses revealed that the serine residue at position 75 modulated ion and ligand interactions. The S75 sidechain coordinated with Mg^{2+} (Fig. 2a, d), but both S75Y and S75L introduced hydrophobic residues which were unable to coordinate Mg^{2+} (Fig. 2b, c), resulting in local packing rearrangements of residues coordinating ligand

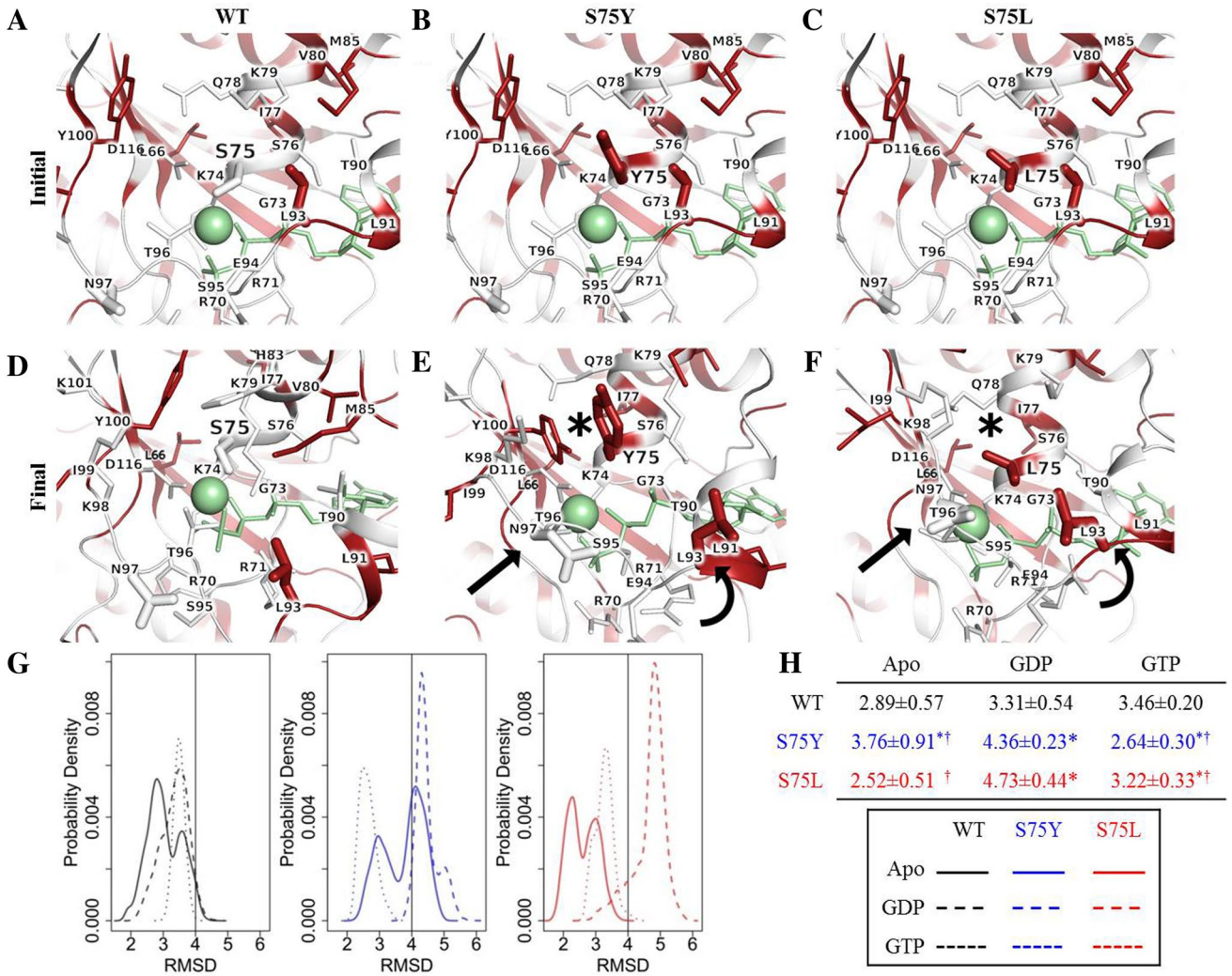

Fig. 2 In silico protein modeling and molecular dynamics simulation of DCM-associated and engineered RagC substitutions. Face-on view of residue 75 and Mg^{2+} coordination in the initial state of **a** WT, **b** S75Y, and **c** S75L and final state of **d** WT, **e** S75Y, and **f** S75L RagC. Residues are colored *white* to *red* according to increasing hydrophobicity. Ligand GTP and Mg^{2+} = *green stick* and *sphere*, respectively; *sticks* sidechain non-hydrogen atoms, *asterisk* rearrangement of residues on the upper face, *curved arrow* movement of α-helix, *straight arrow* compensatory movement of residues to coordinate ligand and Mg^{2+} after loss of S75 interaction. **g** Root mean square deviation (RMSD) density profiles reveal consistent conformational expansion of the GDP-bound form in S75Y and S75L mutants. H RMSD table. Values represent the median ± median absolute deviation. *Asterisk* indicates *p* value <0.05 as compared to corresponding WT-ligand state; †indicates *p* value <0.05 comparing Y75 to L75 (color figure online)

(Fig. 2e, f; asterisks) and within the surrounding area (Fig. 2e, f; curved arrow). Residues in the surrounding area also underwent packing rearrangement to compensate for the loss of S75 coordination with ion and ligand (Fig. 2e, f; straight arrow).

MD trajectories were summarized using RMSD and revealed consistent conformational expansion of the GDP-bound state for both S75Y and S75L (Fig. 2g, h). S75Y also exhibited a greater expansion of the apo form, but stabilization of native-like conformations in the GTP-bound state. By contrast, S75L exhibited expansion of the GTP-bound state. PC analysis revealed mutation-dependent dynamic differences for S75Y and S75L (Figure S1). A significant shift was seen for the GDP-bound form of S75L and the GTP-bound form of both S75Y and S75L (Supplementary Information).

RagC^{S75Y} alters mTORC1 signaling

Due to the predicted GDP-bound expansion of both RagC^{S75Y} and RagC^{S75L}, consistent with mTORC1 activation in reported RagC mutations, we next determined whether S75Y affects mTORC1 activity using a cell culture system. The plasmids expressing empty vector, WT RagC, or RagC^{S75Y} were transfected into human embryonic kidney 293 cells for 48 h. AD293 cells were fasted in medium lacking amino acids/FBS and then re-stimulated in medium with amino acids alone. mTORC1 activity was determined by measuring phosphorylation of p70 S6Kinase (P-S6K) and S6 ribosomal protein (P-S6), a well-established readout of mTORC1 activity (Gressner and Wool 1974). In the fed state, S6K phosphorylation was increased in RagC^{S75Y}, yet there was no difference in the re-fed state between WT

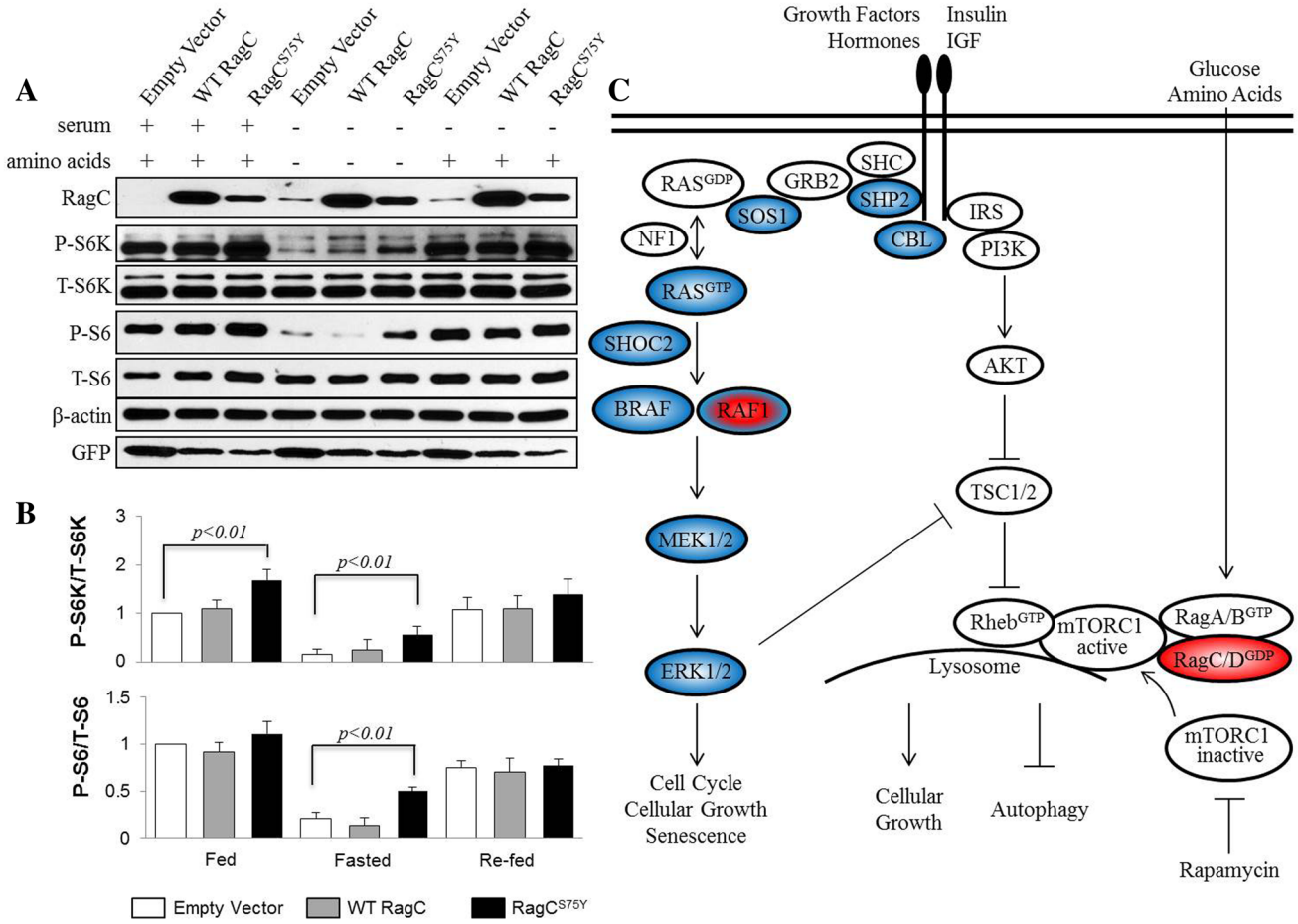

Fig. 3 Impact of RagC^{S75Y} on mTORC1 signaling. **a** Immunoassay showing overexpression of RagC^{S75Y} resulted in increased mTORC1 signaling in the absence of amino acids as compared to wild-type RagC, as indicated by P-S6K and P-S6. AD293 cells overexpressing control-GFP (empty vector) wild-type (WT) RagC or RagC^{S75Y} were starved of amino acids and FBS for 50 min, then re-stimulated in DMEM alone for 20 min. **b** Quantification of P-S6K/T-S6K and P-S6/T-S6 levels from three independent experiments. A significant increase in mTORC1 signaling was seen in cells expressing RagC^{S75Y} compared to WT RagC in the absence of amino acids. **C** Convergence of RAS/MAPK and mTORC1 signaling. *Blue* RAS/MAPK genes associated with hypertrophic cardiomyopathy. *Blue/red* RASopathy gene associated with HCM and non-syndromic DCM. *Red* mTORC1 gene associated with syndromic DCM (color figure online)

RagC and RagC^{S75Y} overexpression (Fig. 3a, b). In both the fed and re-fed states, S6 phosphorylation levels did not differ between WT RagC and RagC^{S75Y} overexpression (Fig. 3a, b). However, amino acid fasting severely reduced S6K and S6 phosphorylation levels in both control cells and cells transfected with WT RagC. By contrast, S6K and S6 phosphorylation levels were increased in cells transfected with RagC^{S75Y} (Fig. 3a, b), indicating that the S75Y mutation rendered cells partially insensitive to amino acid deprivation and resulted in activated mTORC1 signaling.

Discussion

RRAGC and mTORC1 signaling

Mammalian target of rapamycin, mTOR, is an atypical serine/threonine kinase that acts as a master regulator of cell metabolism, growth, proliferation, and survival by forming two multiprotein complexes, mTORC1 and mTORC2, through unique interactions with adaptor proteins (Laplante and Sabatini 2009; Sciarretta et al. 2014). mTORC1, a regulator of cell growth and proliferation, is required for embryonic cardiovascular development and postnatal maintenance of cardiac structure and function (Sciarretta et al. 2014). Stimulation of mTORC1 can occur through multiple mechanisms, including presence of amino acids (Fig. 3c). Amino acid-induced activation of mTORC1 is orchestrated through the four Rag proteins, small guanosine triphosphatases that heterodimerize (RagA or RagB with RagC or RagD) and bind the raptor subunit of mTORC1, thereby promoting activation of mTORC1 by translocation to the lysosomal surface for interaction with its activator, Rheb (Sancak et al. 2008). Stimulation of mTORC1 can also occur through the canonical insulin signaling pathway, and activation of the RAS signaling pathway by growth factors. Specifically, stimulation of RAS/MAPK signaling inactivates TSC1/2, a negative regulator of mTORC1, through increased phosphorylation by AKT and results in activation of mTORC1 (Fig. 3c) (Laplante and Sabatini 2009).

Convergence of RAS/MAPK and AKT/mTORC1 signaling in syndromic cardiomyopathy

RASopathies are clinically distinct developmental syndromes caused by heterozygous germline mutations that perturb the RAS-MAPK pathway and downstream regulation of key cellular processes including cellular growth, differentiation, and senescence (Rauen 2013). The RASopathy Noonan syndrome with multiple lentigines is caused by *PTNPN11* mutations and results in increased AKT-mTORC1 pathway activation (Marin et al. 2011). While hypertrophic cardiomyopathy is a well-established finding in several RASopathies (Gelb et al. 2015), non-syndromic DCM was only recently associated with mutations in the Noonan syndrome gene *RAF1*, wherein rapamycin attenuated downstream AKT-mTOR pathway activation and cardiomyopathy development in a zebrafish model (Dhandapany et al. 2014). Rapamycin treatment has also proved to be beneficial in *Lmna*-deficient mice with enhanced mTORC1 signaling, resulting in improved cardiac and skeletal muscle function (Ramos et al. 2012). Indeed, aberrant mTORC1 activation in cardiomyocytes from patients with nonischemic dilated cardiomyopathy has been associated with myocardial fibrosis and worse prognosis (Yano et al. 2015). In contrast, muscle-specific conditional *Mtor* knockout in mice results in cardiomyocyte loss, due to apoptosis and necrosis, and DCM (Zhang et al. 2014). These findings indicate a delicate balance of mTOR signaling is required in the heart, where perturbations that either increase or decrease signaling can have drastic effects on cardiac physiology. mTORC1 signaling is also critical for autophagy induction in neonates, as demonstrated by expression of a constitutively active RagA mutant (RagA^{Q66L}) in mice that resulted in failure to survive postnatally (Efeyan et al. 2013).

RRAGC is a novel gene for syndromic, fetal DCM

The vast majority of previously reported RASopathy mutations are activating, thereby enhancing RAS/MAPK pathway signaling, yet many of these germline mutations tend to be more weakly activating than their somatic cancer-associated counterparts (Rauen 2013). This distinction in mutation potency has been attributed to intolerance of strongly activating mutations in the germline state or early development (Rauen 2013). These data are consistent with our finding of partial insensitivity of mTORC1 pathway signaling to amino acid deprivation when modeling the RagC^{S75Y} mutation identified in our patient. Interestingly, somatic *RRAGC* mutations were recently found to be enriched in patients with follicular lymphoma, where they clustered in the nucleotide-binding domain of RagC at residues S75, T90, Y115, D116, and P118 (Okosun et al. 2015). When overexpressed in HEK293 cells, the mutations, including S75F, rendered mTORC1 signaling partially or fully insensitive to leucine or arginine deprivation, further validating an essential role of S75 in proper *RRAGC* function and mTORC1 signaling. In conclusion, we used WES to discover a de novo mTORC1-activating mutation in *RRAGC* as a novel molecular basis for sporadic, syndromic DCM. Our findings may lead to improved diagnostic yield of DCM genetic testing in children and provide further rationale to repurpose rapamycin (Kushwaha and Xu 2012), an FDA approved immunosuppressive drug, or develop more targeted rapamycin-related mTORC1

inhibitors for treatment of heart failure due to excessive mTORC1 signaling.

Acknowledgments We thank the family who participated in this study.

Compliance with ethical standards

Conflict of interest The authors declare that they have no conflict of interest.

Funding National Institutes of Health: R01 HL071225 (T.M.O), RO1HL107304 (X.X.), and T32GM072474 (P.A.L.); American Heart Association: 14PRE18070007 (P.A.L.).

Ethical approval This study was approved by the Mayo Clinic Institutional Review Board and all procedures were performed in accordance with the ethical standards of the 1964 Helsinki declaration and its later amendments. Informed consent was obtained from all individual participants included in the study.

References

Adzhubei IA, Schmidt S, Peshkin L, Ramensky VE, Gerasimova A, Bork P, Kondrashov AS, Sunyaev SR (2010) A method and server for predicting damaging missense mutations. Nat Methods 7:248–249. doi:10.1038/nmeth0410-248

Brauch KM, Karst ML, Herron KJ, de Andrade M, Pellikka PA, Rodeheffer RJ, Michels VV, Olson TM (2009) Mutations in ribonucleic acid binding protein gene cause familial dilated cardiomyopathy. J Am Coll Cardiol 54:930–941. doi:10.1016/j.jacc.2009.05.038

DePristo MA, Banks E, Poplin R, Garimella KV, Maguire JR, Hartl C, Philippakis AA, del Angel G, Rivas MA, Hanna M, McKenna A, Fennel TJ, Kernytsky AM, Sivachenko AY, Cibulskis K, Gabriel SB, Altshuler D, Daly MJ (2011) A framework for variation discovery and genotyping using next-generation DNA sequencing data. Nat Genet 43:491–498. doi:10.1038/ng.806

Dhandapany PS, Razzaque MA, Muthusami U, Kunnoth S, Edwards JJ, Mulero-Navarro S, Riess I, Pardo S, Sheng J, Rani DS, Rani B, Govindaraj P, Flex E, Yokota T, Furutani M, Nishizawa T, Nakanishi T, Robbins J, Limongelli G, Hajjar RJ, Lebeche D, Bahl A, Khullar M, Rathinavel A, Sadler KC, Tartaglia M, Matsuoka R, Thangaraj K, Gelb BD (2014) *RAF1* mutations in childhood-onset dilated cardiomyopathy. Nat Genet 46:635–639. doi:10.1038/ng.2963

Efeyan A, Zoncu R, Chang S, Gumper I, Snitkin H, Wolfson RL, Kirak O, Sabatini DD, Sabatini DM (2013) Regulation of mTORC1 by the Rag GTPases is necessary for neonatal autophagy and survival. Nature 493:679–683. doi:10.1038/nature11745

Feig LA, Cooper GM (1988) Inhibition of NIH 3T3 cell proliferation by a mutant *ras* protein with preferential affinity for GDP. Mol Cell Biol 8:3235–3243

Gelb BD, Roberts AE, Tartaglia M (2015) Cardiomyopathies in Noonan syndrome and the other RASoapthies. Prog Pediatr Cardiol 39:13–19

Grant BJ, Rodrigues AP, ElSawy KM, McCammon JA, Caves LS (2006) Bio3d: an R package for the comparative analysis of protein structures. Bioinformatics 22:2695–2696

Gressner AM, Wool IG (1974) The phosphorylation of liver ribosomal proteins in vivo. Evidence that only a single small subunit protein (S6) is phosphorylated. J Biol Chem 249:6917–6925

Hershberger RE, Morales A, Siegfried JD (2010) Clinical and genetic issues in dilated cardiomyopathy: a review for genetics professionals. Genet Med 12:655–667. doi:10.1097/GIM.0b013e3181f2481f

Hershberger RE, Hedges DJ, Morales A (2013) Dilated cardiomyopathy: the complexity of a diverse genetic architecture. Nat Rev Cardiol 10:531–547. doi:10.1038/nrcardio.2013

Irwin JJ, Sterling T, Mysinger MM, Bolstad ES, Coleman RG (2012) ZINC: a free tool to discover chemistry for biology. J Chem Inf Model 52:1757–1768. doi:10.1021/ci3001277

Kumar P, Henikoff S, Ng PC (2009) Predicting the effects of coding non-synonymous variants on protein function using the SIFT algorithm. Nat Protoc 4:1073–1081. doi:10.1038/nprot.2009.86

Kushwaha S, Xu X (2012) Target of rapamycin (TOR)-based therapy for cardiomyopathy: evidence from zebrafish and human studies. Trends Cardiovasc Med 22:39–43. doi:10.1016/j.tcm.2012.06.009

Laplante M, Sabatini DM (2009) mTOR signaling at a glance. J Cell Sci 122(Pt20):3589–3594. doi:10.1242/jcs.051011

Long PA, Evans JM, Olson TM (2015a) Exome sequencing establishes diagnosis of Alström syndrome in an infant presenting with non-syndromic dilated cardiomyopathy. Am J Med Genet A 167A:886–890. doi:10.1002/ajmg.a.36994

Long PA, Larsen BT, Evans JM, Olson TM (2015b) Exome sequencing identified pathogenic and modifier mutations in a child with sporadic dilated cardiomyopathy. J Am Heart Assoc. doi:10.1161/JAHA.115.002443

Mackerell AD Jr, Feig M, Brooks CL 3rd (2004) Extending the treatment of backbone energetics in protein force fields: limitations of gas-phase quantum mechanics in reproducing protein conformational distributions in molecular dynamics simulations. J Comput Chem 25:1400–1415

Marin TM, Keith K, Davies B, Conner DA, Guha P, Kalaitzidis D, Wu X, Lauriol J, Wang B, Bauer M, Bronson R, Franchini KG, Neel BG, Kontaridis MI (2011) Rapamycin reverses hypertrophic cardiomyopathy in a mouse model of LEOPARD syndrome-associated *PTPN11* mutation. J Clin Invest 121:1026–1043. doi:10.1172/JCI44972

McKenna A, Hanna M, Banks E, Sivachenko A, Cibulskis K, Kernytsky A, Garimella K, Altshuler D, Gabriel S, Daly M, DePristo MA (2010) The genome analysis toolkit: a mapreduce framework for analyzing next-generation DNA sequencing data. Genome Res 20:1297–1303. doi:10.1101/gr.107524.110

Michels VV, Moll PP, Miller FA, Tajik AJ, Chu JS, Driscoll DJ, Burnett JC, Rodeheffer RJ, Chesebro JH, Tazelaar HD (1992) The frequency of familial dilated cardiomyopathy in a series of patients with idiopathic dilated cardiomyopathy. N Engl J Med 326:77–82

Nedyalkova L, Tempel W, Tong Y, Crombet L, Zhong N, Guan X, Arrowsmith CH, Edwards AM, Bountra C, Weigelt J, Bochkarev A, Park H, Structural Genomics Consortium (2010) Crystal structure of the nucleotide-binding domain of Ras-related GTP-binding protein C. http://www.rcsb.org/pdb/explore.do?structureId=3LLU. Accessed 26 Feb 2016

Okosun J, Wolfson RL, Wang J, Araf S, Wilkins L, Castellano BM, Escudero-Ibarz L, Al Seraihi AF, Richter J, Bernhart SH, Efeyan A, Iqbal S, Matthews J, Clear A, Guerra-Assunção JA, Bödör C, Quentmeier H, Mansbridge C, Johnson P, Davies A, Strefford JC, Packham G, Barrans S, Jack A, Du MQ, Calaminici M, Lister TA, Auer R, Montoto S, Gribben JG, Siebert R, Chelala C, Zoncu R, Sabatini DM, Fitzgibbon J (2015) Recurrent mTORC1-activating *RRAGC* mutations in follicular lymphoma. Nat Genet 48:183–188. doi:10.1038/ng.3473

Olson TM, Chan DP (2013) Dilated cardiomyopathy. In: Allen HD, Driscoll DJ, Shaddy RE, Feltes TF (eds) Moss and Adams' heart disease in infants, children, and adolescents: including the fetus

and young adult, vol II, 8th edn. Wolters Kluwer Health/Lippincott Williams & Wilkins, Philadelphia, pp 1235–1246

Phillips JC, Braun R, Wang W, Gumbart J, Tajkhorshid E, Villa E, Chipot C, Skeel RD, Kalé L, Schulten K (2005) Scalable molecular dynamics with NAMD. J Comput Chem 26:1781–1802

Pugh TJ, Kelly MA, Gowrisankar S, Hynes E, Seidman MA, Baxter SM, Bowser M, Harrison B, Aaron D, Mahanta LM, Lakdawala NK, McDermott G, White ET, Rehm HL, Lebo M, Funke BH (2014) The landscape of genetic variation in dilated cardiomyopathy as surveyed by clinical DNA sequencing. Genet Med 16:601–608. doi:10.1038/gim.2013.204

Ramos FJ, Chen SC, Garelick MG, Dai DF, Liao CY, Schreiber KH, MacKay VL, An EH, Strong R, Ladiges WC, Rabinovitch PS, Kaeberlein M, Kennedy BK (2012) Rapamycin reverses elevated mTORC1 signaling in lamin A/C-deficient mice, rescues cardiac and skeletal muscle function, and extends survival. Sci Transl Med 4:144ra103. doi:10.1126/scitranslmed.3003802

Rauen KA (2013) The RASopathies. Annu Rev Genomics Hum Genet 14:355–369. doi:10.1146/annurev-genom-091212-153523

Richards CS, Bale S, Bellissimo DB, Das S, Grody WW, Hegde MR, Lyon E, Ward BE, Molecular Subcommittee of the ACMG Laboratory Quality Assurance Committee (2007) ACMG recommendations for standards for interpretation and reporting of sequence variations: revisions 2007. Genet Med 10:294–300. doi:10.1097/GIM.0b013e31816b5cae

Sancak Y, Peterson TR, Shaul YD, Lindquist RA, Thoreen CC, Bar-Peled L, Sabatini DM (2008) The Rag GTPases bind raptor and mediate amino acid signaling to mTORC1. Science 320:1496–1501. doi:10.1126/science.1157535

Sciarretta S, Volpe M, Sadoshima J (2014) Mammalian target of rapamycin signaling in cardiac physiology and disease. Circ Res 114:549–564. doi:10.1161/CIRCRESAHA.114.302022

Sun L, Dimitromanolakis A (2014) PREST-plus identifies pedigree errors and cryptic relatedness in the GAW18 sample using genome-wide SNP data. In: BMC proceedings 8 (Suppl 1 Genetic Analysis Workshop 18Vanessa Olmo) S23. doi:10.1186/1753-6561-8-S1-S23

The 1000 Genomes Consortium (2012) An integrated map of genetic variation from 1092 human genomes. Nature 491:56–65. doi:10.1038/nature11632

Towbin JA, Lowe AM, Colan SD, Sleeper LA, Orav EJ, Clunie S, Messere J, Cox GF, Lurie PR, Hsu D, Canter C, Wilkinson JD, Lipshultz SE (2006) Incidence, causes, and outcomes of dilated cardiomyopathy in children. JAMA 296:1867–1876

Yano T, Shimoshige S, Miki T, Tanno M, Mochizuki A, Fujito T, Yuda S, Muranaka A, Ogasawara M, Hashimoto A, Tsuchihashi K, Miura T (2015) Clinical impact of myocardial mTORC1 activation in nonischemic dilated cardiomyopathy. J Mol Cell Cardiol 91:6–9. doi:10.1016/j.yjmcc.2015.12.022

Zhang P, Shan T, Liang X, Deng C, Kuang S (2014) Mammalian target of rapamycin is essential for cardiomyocyte survival and heart development in mice. Biochem Biophys Res Commun 452:53–59. doi:10.1016/j.bbrc.2014.08.046